

Supplementary Materials for
**Two diphosphorylated degrons control c-Myc degradation by the Fbw7
tumor suppressor**

Markus Welcker, Baiyun Wang, Domnița-Valeria Rusnac, Yasser Hussaini, Jherek Swanger,
Ning Zheng, Bruce E. Clurman*

*Corresponding author. Email: bclurman@fredhutch.org

Published 28 January 2022, *Sci. Adv.* **8**, eab17872 (2022)
DOI: [10.1126/sciadv.ab17872](https://doi.org/10.1126/sciadv.ab17872)

This PDF file includes:

Figs. S1 to S9
Table S1

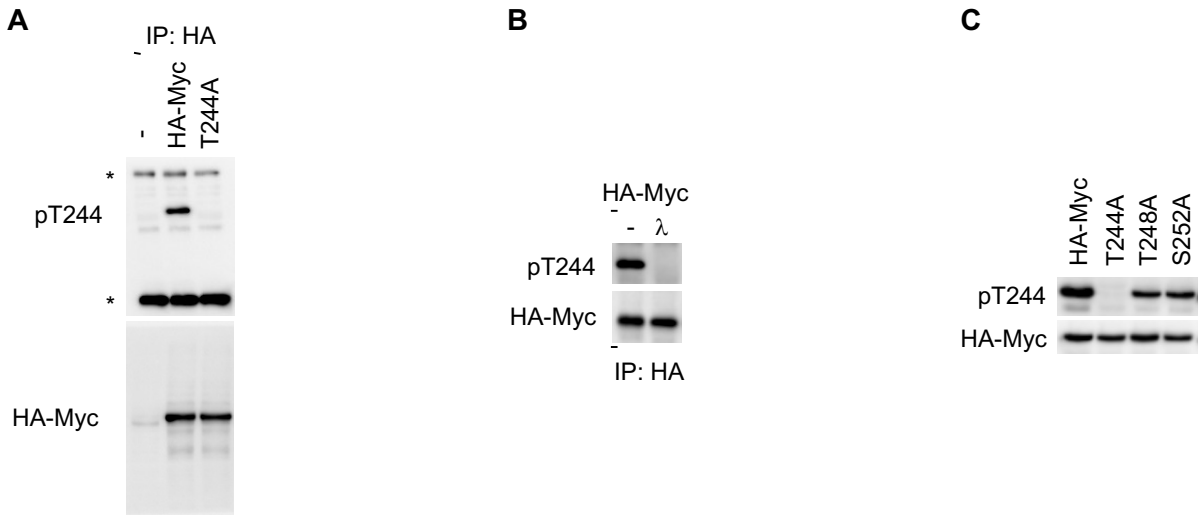


Figure S1

Characterization of the Myc T244 phospho-antibody.

A: HEK293 cells were transfected with HA-Myc or the T244A mutant, lysates immunoprecipitated with HA antibody and blotted for Myc or pT244. The asterisks mark IP antibody chain cross-reactions. **B:** The pT244 antibody is specific to phosphorylation. Immunoprecipitates as in A were treated with lambda phosphatase for 10 minutes before blotting with pT244 antibody. **C:** The pT244 antibody specifically recognizes T244 phosphorylation on overexpressed Myc by direct western blotting of transfected lysates and the epitope appears preserved upon T248 mutation.

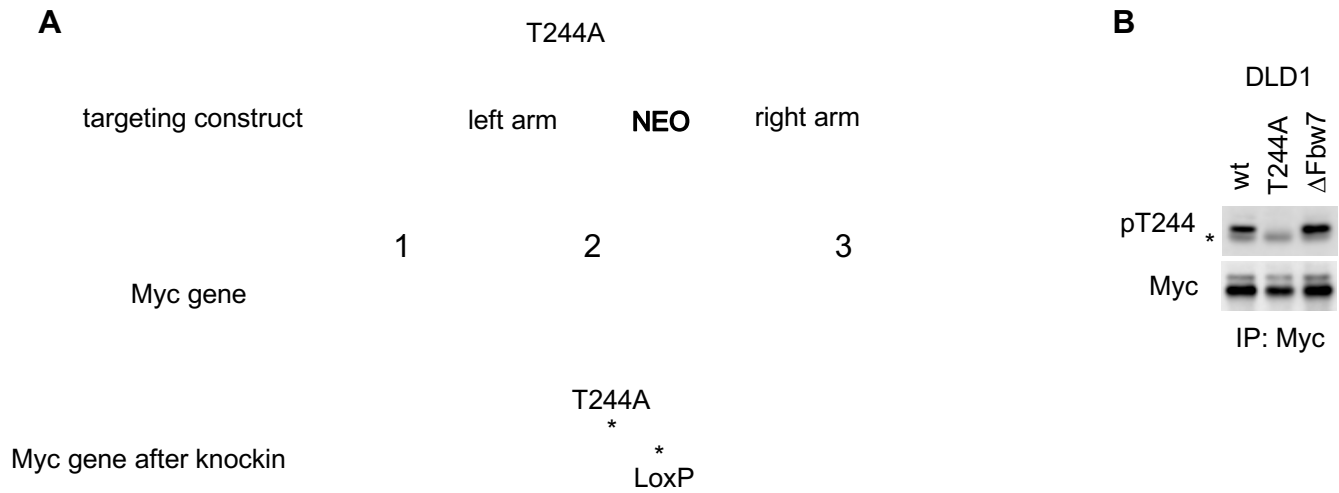


Figure S2

Generation of the T244A homozygous mutation in DLD1 cells.

A: Depiction of the knockin strategy of the T244A mutation. The coding portion of Myc's 3 exons is shown black. T244 is located at the end of exon 2. The targeting construct inserted a selectable marker cassette for neomycin (NEO) into intron 2 along with ~ 1 kb homology arms of the respective genomic Myc sequence on either side, containing the T244A mutation. The NEO cassette was subsequently removed by Cre recombinase, leaving a single LoxP site in intron 2. Clones were validated by both genomic DNA and cDNA sequencing, and by western blot using the pT244 antibody (**B**). Asterisk marks the heavy chain cross-reaction from the IP antibody.

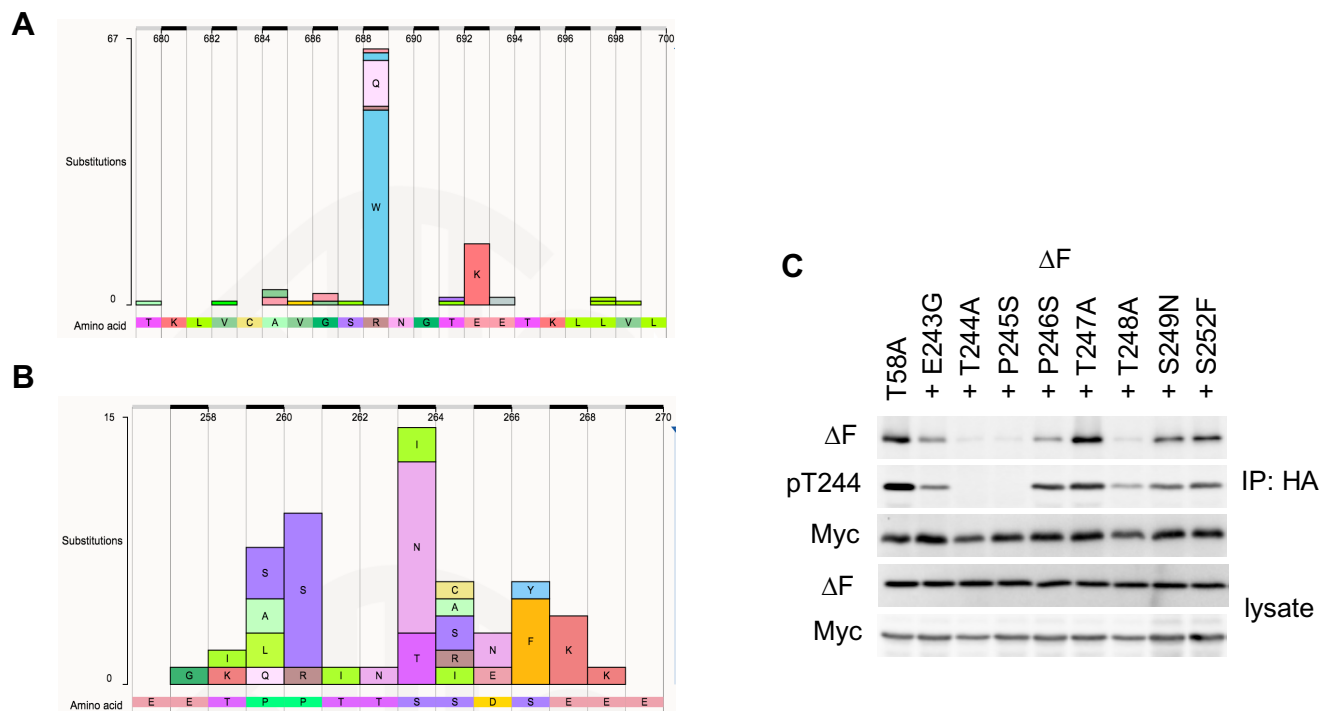


Figure S3

Fbw7 R689 and the Myc T244 degnon are cancer hotspots.

Fbw7 R689 (**A**) and the Myc T244 degnon (**B**) were examined in the COSMIC database (<https://cancer.sanger.ac.uk/cosmic>). **C**: The mutational spectrum of the T244 degnon

(as in B) was tested for effects on Myc T244 phosphorylation and Fbw7 binding.

HEK293 cells were transfected as indicated. All mutations were analyzed in a T58A mutant background to isolate the T244 degnon and binding to Fbw7 was stabilized by F-box deletion. Lysates were immunoprecipitated with HA antibody and blotted as indicated. Note that the pT244 antibody epitope recognition is likely affected by proximal mutations. Besides the T244 and T248 phosphorylation sites, P245 is most critical for Fbw7 interaction (and perhaps T244 phosphorylation), while E243 and P246 also contribute to Fbw7 binding. S249 and S252 mutations likely affect proper kinase targeting for the core degnon phosphorylation sites.

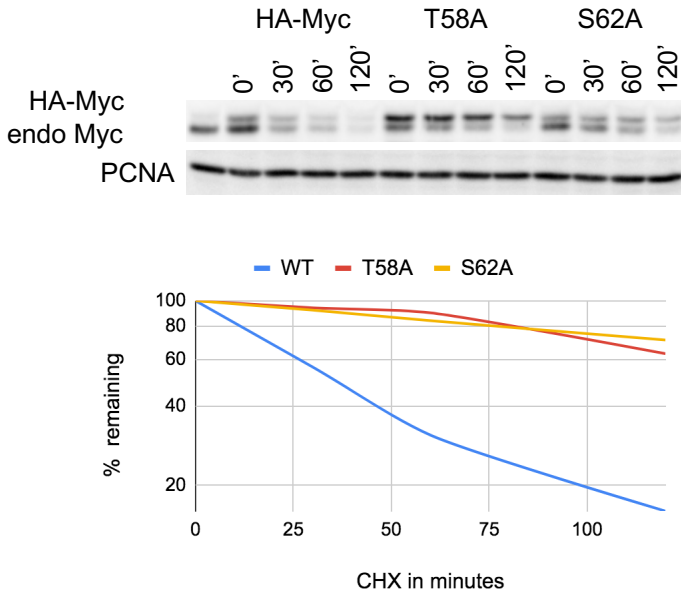


Figure S4

Myc S62 phosphorylation destabilizes Myc.

U2OS cells were transfected with low levels of HA-Myc or its phosphorylation site mutants T58A and S62A (100 ng per 6 cm dish) to resemble physiologic amounts of Myc expression. Identical samples were subjected to cycloheximide chases for the indicated times in minutes and analyzed by immunoblotting with Myc antibody. The exogenous Myc migrates just above endogenous protein due to its HA-tag. The first lane is an untransfected sample to indicate the migration of endogenous Myc. PCNA serves as loading control. Bands were quantified and plotted below.

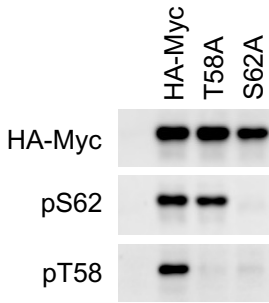
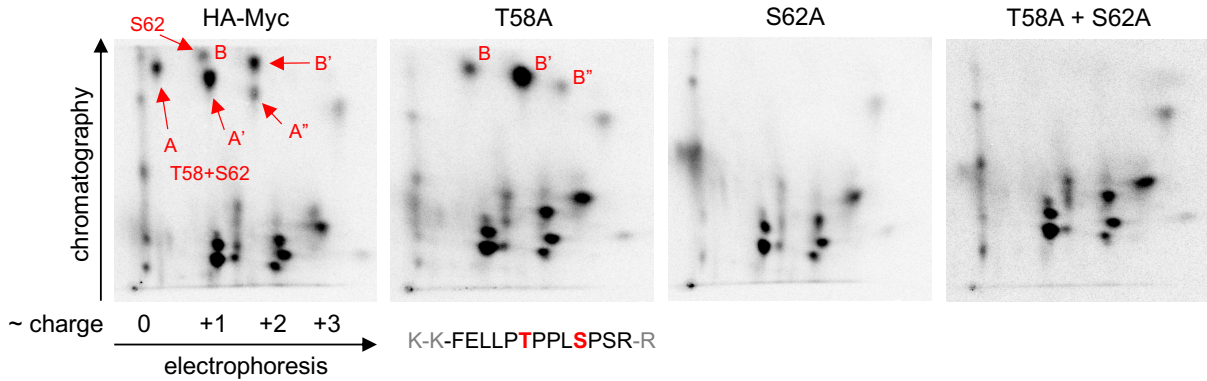
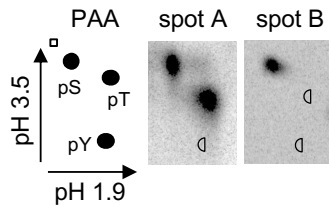


Figure S5

Specificity test of commercial Myc phospho-antibodies.

Myc or phosphorylation-site mutants were transfected into HEK293 cells and lysates separately blotted as indicated. The lack of pT58 signal in the S62A mutants reflects its priming dependence by GSK3. Note that alanine mutation of S62 does not affect the epitope recognition by the pT58 antibody (see Figure 3D).

A**B****Figure S6****Definition of the localization of the tryptic pT58/pS62 peptide in 2D analysis.**

A: HA-Myc or the indicated mutants were transfected into HEK293 cells, labeled with orthophosphate and lysates immunoprecipitated against the HA tag. Myc was subjected to 2D phospho-peptide mapping followed by phospho-amino acid analysis to identify the localization of pT58 and pS62. The di-phosphorylated peptide A as well as the S62 single phosphorylated peptide B are displayed in multiple spots due to partial digestion on either end of this peptide (displayed below T58A map). We could not identify T58-only phosphorylated peptides, consistent with other published Myc phospho-peptide maps. Based on our experience with cyclin E, where S384 phosphorylation prevents

downstream trypsin cleavage at K386 and cuts at K387 instead (30), S62 phosphorylation may similarly prevent efficient tryptic cleavage at the downstream R65, cleaving at R66 instead. This adds one arginine residue to the peptide, shifting spot A to the A' position as addition of a positive charge expectedly moves the peptide to the right and slightly lower (for hydrophobic peptides). The appearance of spot A" is most likely due to inefficient cleavage at the N-terminal lysine residues of this peptide (K51/K52) again adding a positive charge to the peptide, shifting the peptide further to the right and again lower. In the absence of T58 phosphorylation (T58A panel) spot A disappears and is instead shifted into spot B (pS62 only). Both spots are eliminated upon S62 mutation (S62A or T58A+S62A), consistent with the priming function of pS62 for T58 phosphorylation. The additional spots in the lower half of the map are other reported phosphorylations. T244 phosphorylation is not detected by this analysis, likely due to the large and acidic nature of this peptide. **B:** All marked spots were eluted and subjected to phospho-amino acid analyses (PAA), demonstrating the equal presence of both phospho-serine and phospho-threonine in spot A, while spot B only contained phospho-serine.

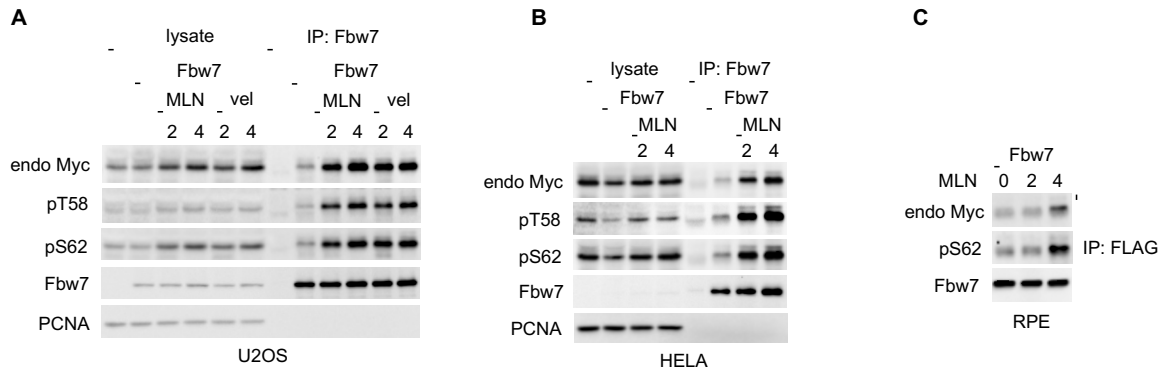


Figure S7

S62 is efficiently phosphorylated in Fbw7 complexes in a variety of cell lines.

U2OS cells (**A**), HELA cells (**B**), and RPE cells (**C**) were assayed as in Figure 4F. U2OS cells were alternatively treated with the proteasome inhibitor velcade (vel) or MLN4924 for the indicated hours. Note that pS62 accumulated in Fbw7 complexes with similar kinetics as Myc in general. PCNA serves as loading control.

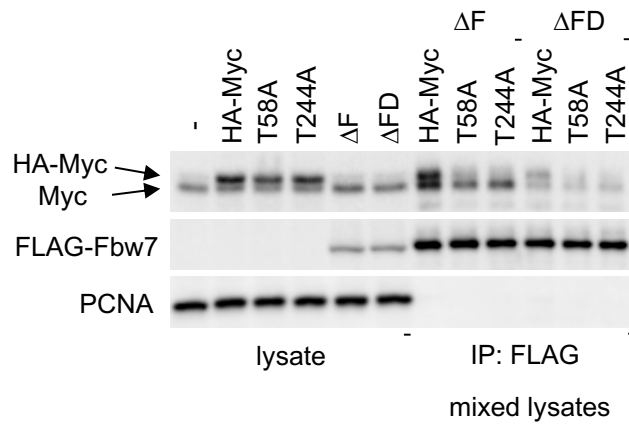


Figure S8

Myc and Fbw7 complex formation from separately transfected cell lysates.

This experiment complements Figures 5E and 5F, only that the assay was done by separate Myc and Fbw7 transfections and lysates were subsequently mixed for immunoprecipitation. Input lysates shown on the left, immunoprecipitation of mixed lysates on the right. Exogenous HA-Myc migrates just above the endogenous Myc protein.

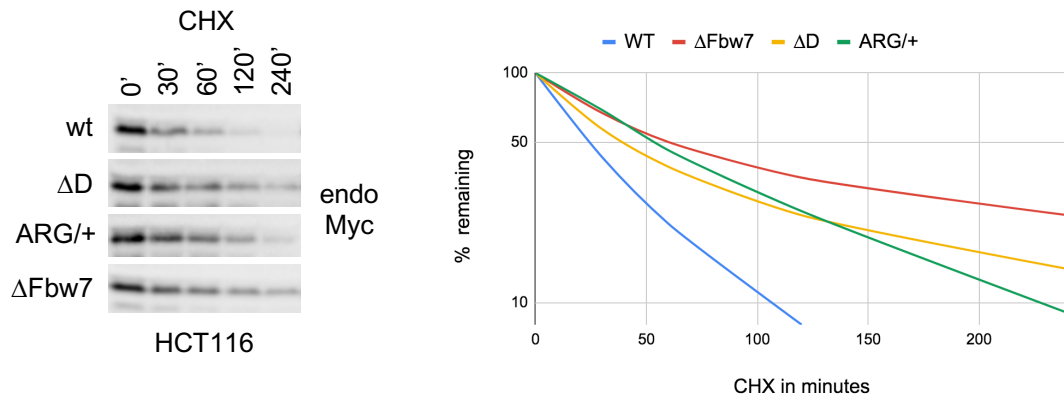


Figure S9

Myc is stabilized in HCT116 cells engineered to express endogenous Fbw7 dimerization mutants (Δ D) or a heterozygous ARG mutant.

HCT116 cells or their gene-targeted isogenic mutant lines were subjected to cycloheximide chases (time in minutes) and immunoblotted for endogenous Myc protein. Quantification is plotted on the right.

Table S1. Data collection and refinement statistics (molecular replacement)

	FBW7-Myc-N-degron	FBW7-Myc-C-degron
Data collection		
Space group	I4122	I4122
Cell dimensions		
<i>a</i> , <i>b</i> , <i>c</i> (Å)	232.87, 232.87, 107.16	232.54, 232.54, 107.84
α , β , γ (°)	90.00, 90.00, 90.00	90.00, 90.00, 90.00
Resolution (Å)	50.0-2.77 (2.82-2.77)	50.0-2.55 (2.59-2.55)
<i>R</i> _{sym} or <i>R</i> _{merge}	.198 (1.445)	.126 (1.134)
<i>I</i> / σ <i>I</i>	12.00 (1.16)	19.11 (1.14)
Completeness (%)	100.0 (100.0)	99.7 (96.3)
Redundancy	9.7 (8.5)	9.5 (6.2)
Refinement		
Resolution (Å)	49.96-2.77	49.98-2.55
No. reflections	37654	48054
<i>R</i> _{work} / <i>R</i> _{free}	22.47/24.97	25.30/26.77
No. atoms	4703	4683
Protein	4579	4595
Ligand/ion	25	15
Water	99	73
<i>B</i> -factors		
Protein	56.51	60.69
Ligand/ion	67.85	78.31
Water	44.58	50.73
R.m.s. deviations		
Bond lengths (Å)	0.026	0.010
Bond angles (°)	1.404	1.396
Ramachandran		
Allowed (%)	8.14	7.26
Favored (%)	91.50	92.39
Disallowed (%)	0.35	0.35